

# Stabilized jellium model and the equilibrium properties of simple metal thin films

T. Mahmoodi

*Physics Department, Islamic Azad University, Mash'had Branch, Iran.*

M. Payami\*

*Physics Group, Nuclear Science and Technology Research Institute,  
Atomic Energy Organization of Iran, Tehran, Iran.*

(Dated: May 2, 2019)

In this work, we have applied the self-compressed stabilized jellium model to predict the equilibrium properties of isolated thin Al, Na, and Cs slabs. Our results show that the equilibrium  $r_s$  value when the number of particles is constant is different from that when the volume of the slab is kept constant. To make a direct correspondence to atomic slabs, we have considered only those  $L$  values that correspond to  $n$ -layered atomic slabs with different ( $hkl$ ) surfaces. Our results show that the quantum size effects are significant for slabs with  $L$  smaller or near to  $\lambda_F$ . We have shown that some slabs relax to larger  $L$  values while others compress with respect to the bulk spacings, consistent with already *ab. initio.* predictions. However, the self-compressed calculations on metal clusters have shown that relaxations were only compressions. Moreover, it is shown that in the slab systems, in contrast to the case of metal clusters, the  $E/N$  as a function of  $n$  converge to bulk value from above. Our results for large  $n$  values are in good agreement with those already obtained in semi-infinite stabilized jellium calculations.

PACS numbers: 73.43.Nq, 71.15.-m, 73.22.-f, 73.43.Cd, 73.21.Fg

## I. INTRODUCTION

A thin slab is a system composed of a few atomic layers in such a way that it is finite in one direction (here we take as  $z$  axis), and infinite in the other two directions of  $x$  and  $y$ . The finiteness of the size in the  $z$  direction gives rise to the so-called quantum-size effects (QSE).<sup>1,2,3</sup> The QSEs are significant when the size,  $L$ , of the system in one direction is comparable to the Fermi wavelength,  $\lambda_F$ , of the electron in that direction and become less important in the limit  $L \gg \lambda_F$ .

It has been shown that the stabilized jellium model (SJM)<sup>4</sup> is a simple and realistic model to describe the bulk properties of simple metals. Moreover, it is well-known that the self-compressed (SC) version of the SJM (abbreviated with SJM-SC) is appropriate for finite systems in which the surface effects causes the jellium background density differ from that of the bulk.<sup>5,6,7</sup> In the prior work by Sarria *et. al.*,<sup>3</sup> the SJM-SC has been applied for slabs with different widths of  $L$ . For each  $L$  value, they have determined that  $r_s^*$  for the background which minimized the total energy per particle ( $E/N$ ). That procedure was repeated for various  $L$  values, taking  $L$  as a continuous parameter. They have shown that for certain values of parameter  $L$  which are integer multiples of  $\lambda_F/2$ , the self-compression effects are more pronounced. However, since the self-compression procedure was performed for constant  $L$  values, any change of the  $r_s$  value was equivalent to change in the number of atoms and thereby, the slab systems would not be isolated systems anymore. In order to apply the SJM-SC for isolated

slabs, we have to consider  $N$  as a fixed parameter and let the value of  $L$  relax to its equilibrium value  $L^\dagger$ . The relaxation of  $L$  relative to the corresponding bulk value leads to a change in the  $r_s$  to keep  $N$  fixed. We denote by  $r_s^\dagger$  the value corresponding to the  $L^\dagger$ .

In this work, using the SJM-SC, we have calculated the equilibrium properties of isolated thin slabs of simple metals Al, Na, and Cs. The calculations are based on the density functional theory (DFT)<sup>8</sup> and solution of the Kohn-Sham (KS) equations<sup>9</sup> in the local density approximation (LDA)<sup>9</sup> for the exchange-correlation (XC) functional. In our calculations, as mentioned above, the slabs are taken as isolated systems which can undergo relaxations in the  $z$  direction. Our results show that, in contrast to the  $r_s^*$ , the  $r_s^\dagger$  is not always less than the bulk value. This means that in some cases the relaxations are expansions. This behavior is in agreement with the first-principles calculations.<sup>10,11,12,13</sup> We have derived the relation between  $r_s^*$  and  $r_s^\dagger$  which is presented in Appendix.

The organization of this paper is as follows. In section II we explain the calculational details. Section III is devoted to the results of our calculations and finally, we conclude this work in section IV.

## II. CALCULATIONAL DETAILS

In the SJM-SC, the energy of a system with electronic charge distribution  $n(\mathbf{r})$  and background charge  $n_+(\mathbf{r})$  is given by:<sup>5,14</sup>

$$E_{\text{SJM}}[n, n_+] = E_{\text{JM}}[n, n_+] + [\varepsilon_{\text{M}}(r_s) + \bar{w}_R(r_s, r_c)] \int d\mathbf{r} n_+(\mathbf{r}) + \langle \delta v \rangle_{\text{WS}}(r_s, r_c) \int d\mathbf{r} \Theta(\mathbf{r}) [n(\mathbf{r}) - n_+(\mathbf{r})], \quad (1)$$

where,  $E_{\text{JM}}$  is the energy in the jellium model (JM),<sup>15</sup>  $\varepsilon_{\text{M}} = -9z/10r_0$  and  $\bar{w}_R = 2\pi\bar{n}r_c^2$  are the Madelung energy and the average of the repulsive part of the pseudopotential<sup>16</sup> over the Wigner-Seitz (WS) cell of radius  $r_0 = z^{1/3}r_s$ , respectively.  $z$  and  $\langle \delta v \rangle_{\text{WS}} = (3r_c^2/2r_s^3 - 3z/10r_0)$  are the valency of the atom and the average of the difference potential over the WS cell, respectively.<sup>4</sup>  $n_+(\mathbf{r}) = \bar{n}\Theta(\mathbf{r})$  is the jellium density in which  $\bar{n} = 3/4\pi r_s^3$  and  $\Theta(\mathbf{r})$  takes the value of unity inside the jellium background and zero outside.  $r_c$  is the core radius of the pseudopotential and is determined in such a way that the bulk system becomes mechanically stabilized at the experimental  $r_s$  value. Here, we have used the Hartree atomic units throughout the paper. For a finite system (with fixed number of particles) at mechanical equilibrium, the  $r_s$  value of the background is different from the bulk value and assumes the value  $r_s^\dagger$  for which

$$\left. \frac{\partial(E/N)}{\partial r_s} \right|_{r_s^\dagger} = 0, \quad (2)$$

where  $N$  is the number of electrons in the system.

In the SJM-SC, a slab of thickness  $L$  has a full translational symmetry in the  $x$  and  $y$  directions, and therefore, the physical quantities depend on the spacial  $z$  coordinate. Moreover, the KS equation reduces to a one-dimensional equation,

$$\left( -\frac{1}{2} \frac{d^2}{dz^2} + v_{\text{eff}}(z) \right) \psi_n(z) = \varepsilon_n \psi_n(z), \quad (3)$$

where

$$v_{\text{eff}}(z) = \phi(z) + v_{\text{xc}}(z) + \langle \delta v \rangle_{\text{WS}} \Theta(L/2 - |z|). \quad (4)$$

$\phi(z)$  is the electrostatic potential energy,

$$\phi(z) = 4\pi \int_{-\infty}^z dz' (z - z') [n_+(z') - n(z')], \quad (5)$$

satisfying  $\phi(\pm\infty) = 0$ , and the density is given by:<sup>1</sup>

$$n(z) = \frac{1}{\pi} \sum_{\varepsilon_n \leq E_{\text{F}}} (E_{\text{F}} - \varepsilon_n) \phi_n^2(z), \quad (6)$$

with the Fermi energy determined by the charge neutrality condition

To solve the KS equation for a slab of width  $L$ , we expand the KS orbitals in terms of the eigenfunctions of a rectangular infinite potential well<sup>2</sup> of width  $D \approx L + 4\lambda_{\text{F}}$ , which allows a  $2\lambda_{\text{F}}$  vacuum at each side of the slab. Our experience shows that this choice of the width

TABLE I: Interlayer spacings in terms of lattice constant for different structures.

structure	$d_{100}$	$d_{110}$	$d_{111}$
fcc	$\frac{a}{2}$	$\frac{a}{2\sqrt{2}}$	$\frac{a}{\sqrt{3}}$
bcc	$\frac{a}{2}$	$\frac{a}{\sqrt{2}}$	$\frac{a}{2\sqrt{3}}$

$D$  works well in most cases and ensures the convergency with respect to  $D$ .

For an  $X(hkl)$  slab ( $X=\text{Al, Na, Cs}$ ) composed of  $n$  atomic layers, we have  $L = nd_{hkl}$ , with  $d_{hkl}$  being the interlayer spacing. For a unit cell of  $n_{\text{at}}$  atoms with valency  $z$ , the lattice constant  $a$  is determined from the electronic  $r_s$  value by  $a = (4\pi z n_{\text{at}}/3)^{1/3} r_s$ . Knowing the fact that  $n_{\text{at}}$  is four for a face centered cubic (fcc), and is two for a body centered cubic (bcc) structures, we have summarized, in Table I, the relations between the lattice constants  $a$  and interlayer spacings  $d_{hkl}$  for each structure. For Al, Na, and Cs we have used the bulk  $r_s$  values of 2.07, 3.99, and 5.63, respectively. In Table II we have presented the numerical bulk values of  $a$  and  $d_{hkl}$  for each element. It should be mentioned that since  $\lambda_{\text{F}} = 2\pi(4/9\pi)^{1/3} r_s$  also scales with  $r_s$ , the lattice constant in units of Fermi wavelength depends only on the valency of the atoms and the crystal structure, *i.e.*,  $a = (3z n_{\text{at}}/8\pi)^{1/3} \lambda_{\text{F}}$ . To proceed with SJM-SC calculations for an isolated slab, we must determine how  $r_s$  is related to  $L$ . Since in the  $x$  and  $y$  directions there is no relaxations, the surface area of the slab remains constant and the change in  $r_s$  is solely due to the change in  $L$ . That is,

$$L^\dagger = \left( \frac{r_s^\dagger}{r_s} \right)^3 L, \quad (7)$$

where the pairs  $(L^\dagger, r_s^\dagger)$  and  $(L, r_s)$  correspond to the equilibrium and bulk states of the slab.

### III. RESULTS AND DISCUSSION

Using the SJM-SC and solution of the KS equations, we have calculated the equilibrium sizes,  $L^\dagger$ , of  $n$ -layered slabs ( $2 \leq n \leq 20$ ) for Al, Na, and Cs. For each element, the  $n$ -layered slab calculations has been repeated for the different (100), (110), and (111) surfaces. Here, the differences in the surfaces is just in the interlayer spacings. The advantages of using different  $d_{hkl}$  is that we just consider those  $L$  values that correspond to real atomic slabs and therefore, the results are directly connected to atomic slabs. For each isolated slab, we have solved the

TABLE II: Bulk values of lattice constants and interlayer spacings in atomic units. The values in parentheses are in units of bulk Fermi wavelength,  $\lambda_F$ .

element	structure	$a$	$d_{100}$	$d_{110}$	$d_{111}$
Al	fcc	7.64 (1.13)	3.82 (0.56)	2.70 (0.40)	4.41 (0.65)
Na	bcc	8.10 (0.62)	4.05 (0.31)	5.73 (0.44)	2.34 (0.18)
Cs	bcc	11.43 (0.62)	5.72 (0.31)	8.08 (0.44)	3.30 (0.18)

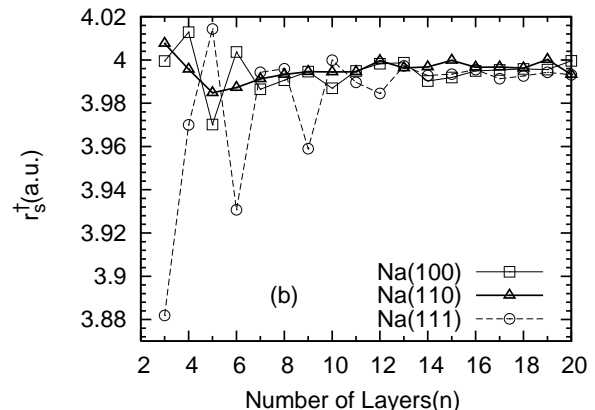
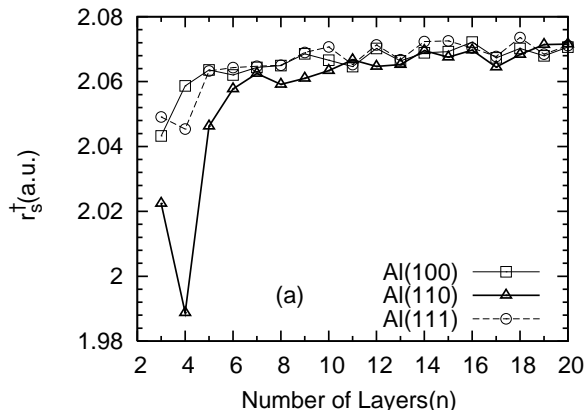


FIG. 1: Equilibrium  $r_s$  values, in atomic units, for  $n$ -layered slabs with (100), (110), and (111) surfaces. (a), (b), and (c) correspond to Al, Na, and Cs, respectively.

KS equations for different  $r_s$  values and have determined the  $r_s^\dagger$  which minimized  $E/N$ .

In Fig. 1 (a), we have plotted the  $r_s^\dagger$  for Al(100), Al(110), and Al(111) as function of the number of atomic layers,  $n$ . The results show that in Al(100), the slabs with  $n=12, 16, 18,$  and  $20$  slightly expand relative to their bulk values. The same situation in Al(110) is observed for  $n=19, 20$ ; and in Al(111) for  $n=10, 12, 14, 15, 16, 18,$  and  $20$ . For other  $n$  values, the relaxations are as compressions. For Na and Cs, the results are plotted in Figs. 1 (b) and (c), respectively. In the case of Na(100), all  $n$  values (except for  $n=5, 7, 10$ ) show expansions, in Na(110), all  $n$  values (except for  $n=5, 6$ ) show expansions, and in Na(111), all  $n$ s (except for  $n=3, 4, 6, 9, 11, 12$ ) show expansions. In the Cs case, almost all slabs show expansions except for  $n=5$  in (100) and  $n=3, 4, 6, 9$  in (111). It is seen that the amplitude of QSE oscillations are more pronounced for slabs with  $d_{hkl} \ll \lambda_F$  [See, for example, Na(111) and Cs(111)], and in cases where  $L$  becomes integer multiples of  $\lambda_F/2$ . The oscillations in Na and Cs are more or less the same because their interlayer spacings are the same (in units of  $\lambda_F$ ) but their pseudopotential core radii are different (See Fig. 1 of Ref. 14 and Table I of Ref. 4), which can be the origin of small differences.

The relative changes in the  $r_s$  values,  $(r_s^\dagger - r_s)/r_s$ , are plotted in Figs. 2 (a)-(c). The results should be compared with those plotted in Fig. 6 of Ref. 3. The comparison reveals the differences in the values of  $r_s^*$  (Ref. 3) and

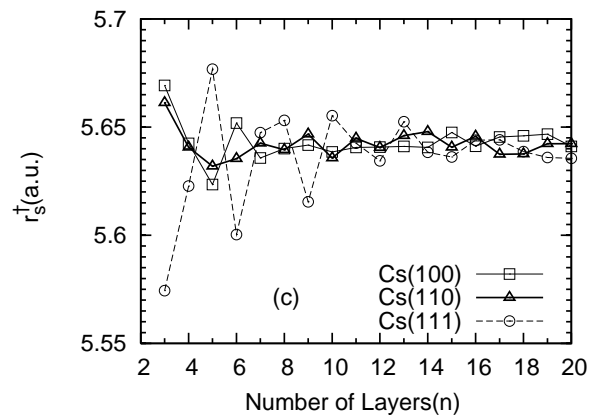


Fig. 1 (Continued)

$r_s^\dagger$ . In Appendix, we have derived, in detail, the relation between these two quantities. Moreover, it should be mentioned that the relative changes in  $r_s$  for Cs is smaller than those of Al and Na.

Using Eq. (7), the  $L^\dagger$ s are calculated and the  $(L^\dagger - L)/L$  results are plotted in Figs. 3 (a)-(c). Since, the relative changes in  $r_s$  and  $L$  are related by

$$\frac{\Delta r_s}{r_s} = \left( \frac{\Delta L}{L} \right)^{1/3} - 1, \quad (8)$$

the behavior for small relaxations would be the same (within a multiplicative factor) as in Figs. 2.

We have plotted, in Figs. 4 (a)-(c), the Fermi energies as functions of the number of layers for Al, Na, and Cs, respectively. The Fermi energy is the minus of the minimum energy needed to remove an electron from inside of the slab. As  $n$  increases, it approaches the minus work function of the corresponding semi-infinite metal

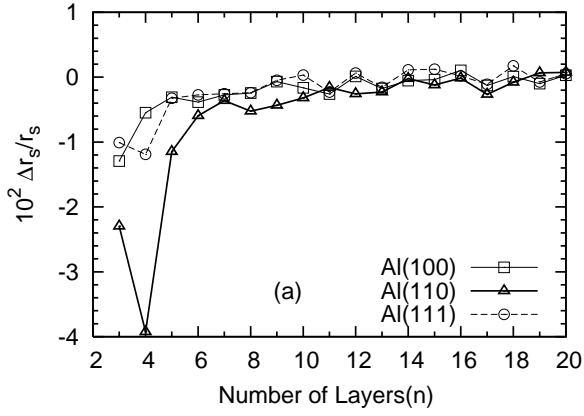


FIG. 2: Relative changes of the equilibrium  $r_s$  with respect to the bulk values. (a), (b), and (c) correspond to Al, Na, and Cs, respectively.

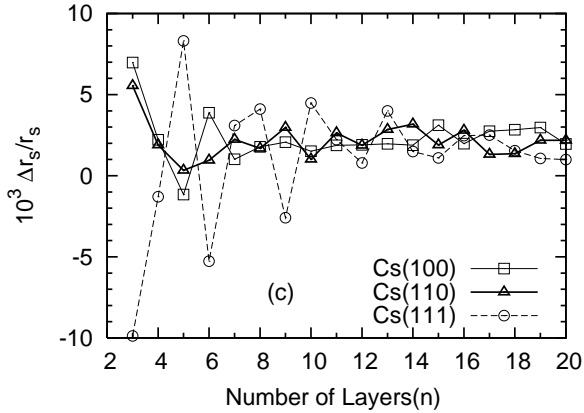
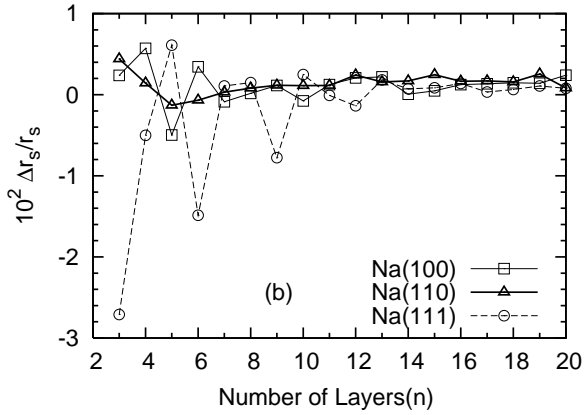


Fig. 2 (Continued)

(See Table IV of Ref. 4).

The total energies per electron,  $E/N$ , at corresponding  $r_s^\dagger$  values are plotted as functions of  $n$  in Figs. 5 (a)-(c) for Al, Na, and Cs, respectively. As in the above plots, for large  $n$ , the semi-infinite values are approached. However, for small  $n$  values, the plots of (100), (110), and (111) are distinct. The upper curve corresponds to slabs with lowest interlayer spacing which is (110) for Al, and (111) for both Na and Cs. The plots show the main

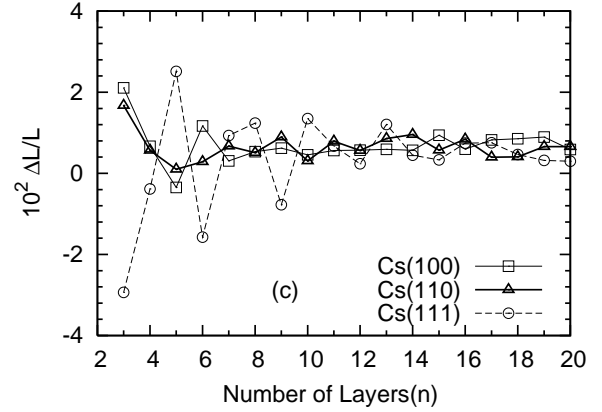
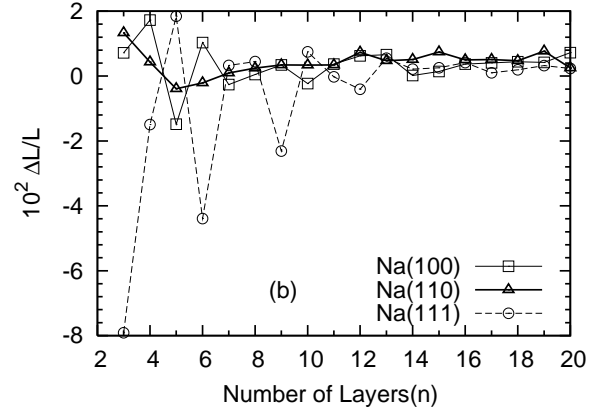
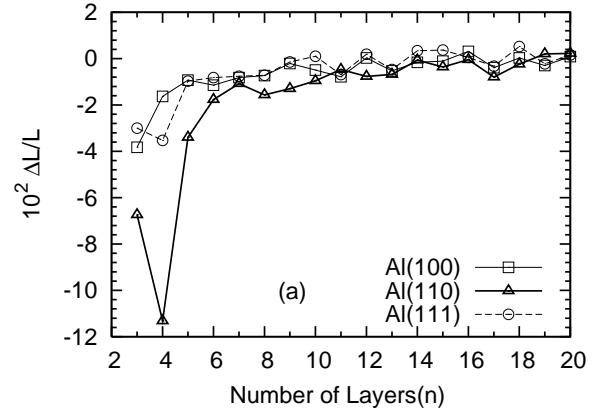


FIG. 3: Relative change in the slab width as function of  $n$  (a) for Al, (b) for Na, and (c) for Cs.

difference in the behaviors of  $E/N$  for self-compressed metal slabs and self-compressed metal clusters.<sup>5</sup> In the metal cluster case, the plots approach to the bulk value from below (more negative) whereas in slabs it is from above (less negative).

The surface energy of the slab is defined by

$$\sigma(L^\dagger) = \frac{1}{2A} [E_{\text{SJM}}(L^\dagger) - E_{\text{SJM}}^{\text{bulk}}(L)], \quad (9)$$

where  $E_{\text{SJM}}(L^\dagger)$  and  $E_{\text{SJM}}^{\text{bulk}}(L)$  are the SC-SJM and bulk-SJM total energies of the slab with surface area  $A$ . The bulk-SJM total energy is proportional to  $L = nd_{hkl}$  and

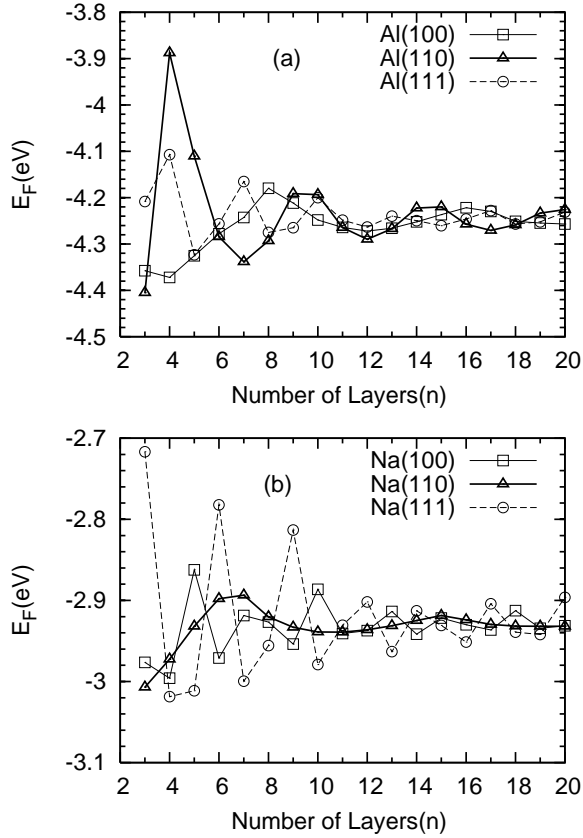


FIG. 4: Fermi energies, in units of eV, as functions of  $n$  (a) for Al, (b) for Na, and (c) for Cs, respectively. As is seen, for large  $n$  values, the (100), (110), and (111) plots approach the value of semi-infinite system.

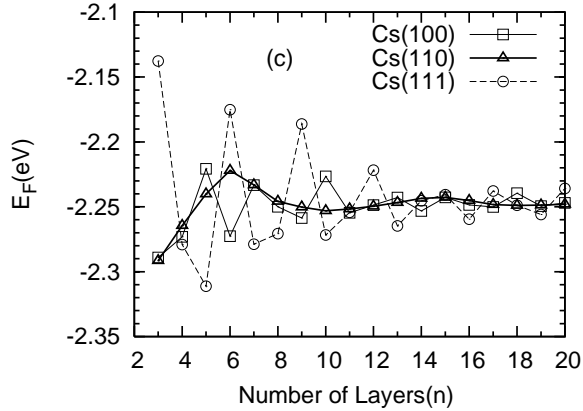


Fig. 4 (Continued)

Eq. (9) can be rewritten in the form of

$$\frac{E_{\text{SJM}}(L^\dagger)}{A} = 2\sigma(L^\dagger) + L\bar{n}\varepsilon^{\text{bulk}}, \quad (10)$$

where  $\bar{n}$  and  $\varepsilon^{\text{bulk}}$  are the bulk density and bulk SJM energy per particle, respectively. We have fitted the values of the SC-SJM total energy per unit area to Eq. (10) to obtain  $\varepsilon^{\text{bulk}}$ , and used it in Eq. (9) to obtain  $\sigma(L^\dagger)$ . In

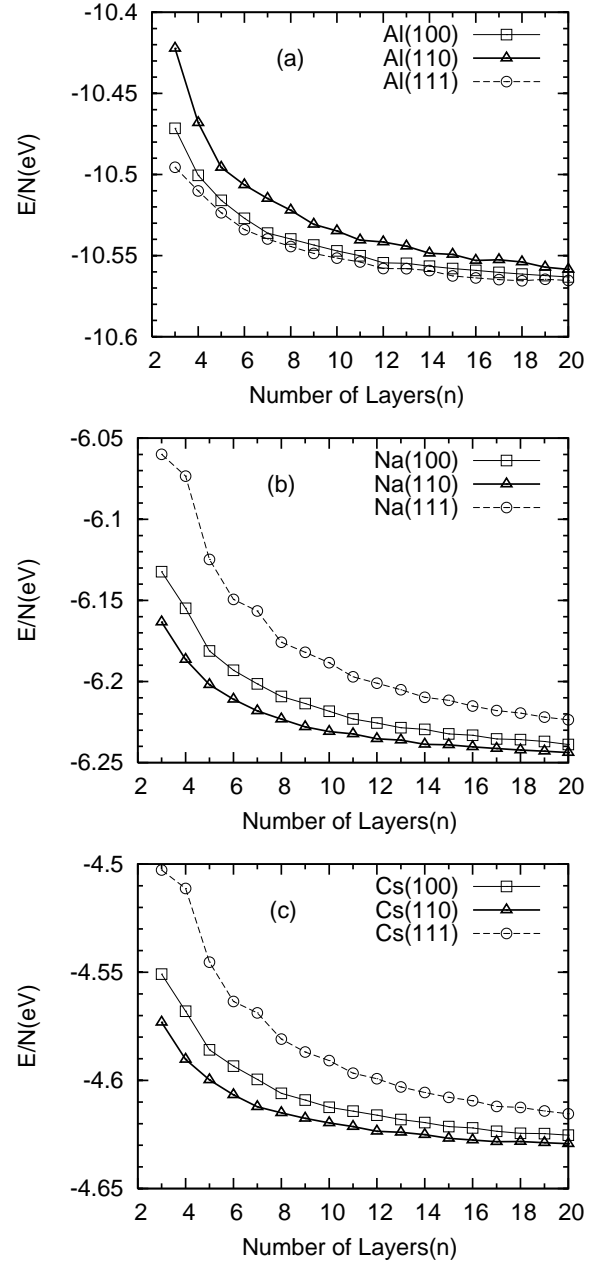


FIG. 5: Total energies per electron at  $r_s^\dagger$ , in eV, (a) for Al, (b) Na, and (c) Cs, respectively. In contrast to metal clusters, it is approached to the bulk value from above.

the fitting we have used the results with  $n \geq 6$  to obtain more accurate values for  $\varepsilon^{\text{bulk}}$ . The results are plotted in Figs. 6 (a)-(c). The values well converge to those of corresponding semi-infinite stabilized jellium systems.<sup>4</sup> However, in the Al case, our results for  $E_F$  and  $\sigma$  show small deviations from the semi-infinite values. This is because, we have treated Al as equivalent mono-valent atom with three WS cells of radius  $r_s$  and ion charge  $z^* = 1$  for each atom.<sup>4</sup>

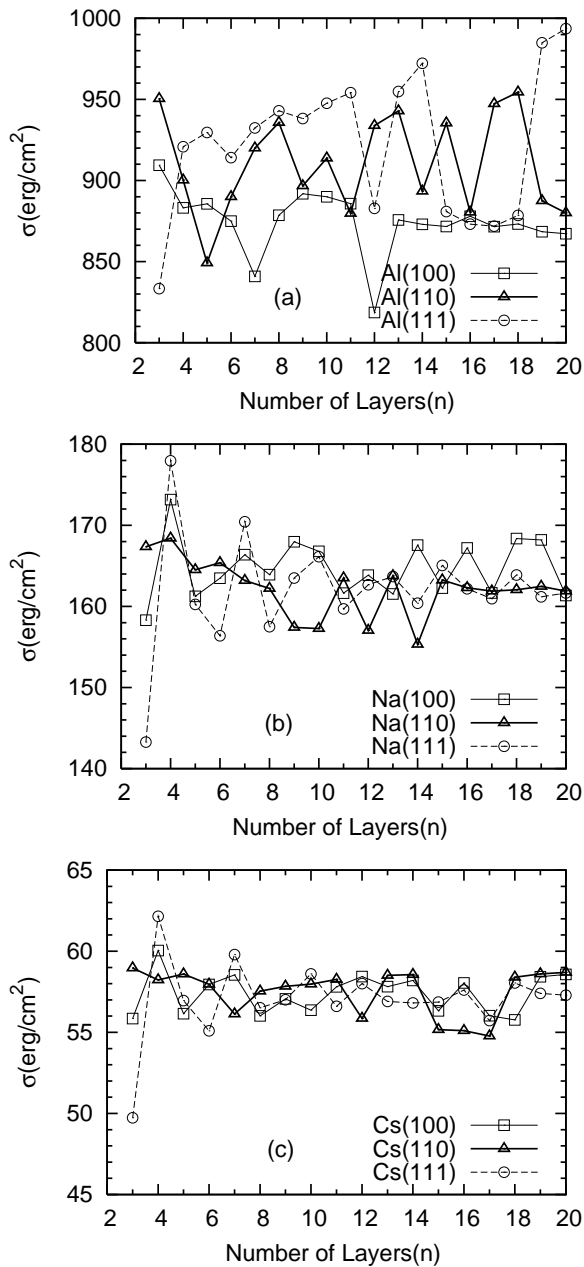


FIG. 6: Surface energies in units of  $\text{erg}/\text{cm}^2$  for (a) Al, (b) Na, and (c) Cs, respectively.

#### IV. CONCLUSIONS

We have applied the SC-SJM to isolated slabs of Al, Na, and Cs. We have shown that the equilibrium  $r_s$  value when the number of particles are constant is different from that when the volume of the slab is kept constant. In our calculations, we have considered only those  $L$  values that correspond to  $n$ -layered atomic slabs with different  $(hkl)$  surfaces. The results show that the QSEs are significant for slabs with  $L \approx \lambda_F$  or smaller. Our results show that some slabs relax to larger  $L$  val-

ues whereas others compress. This behavior has been already predicted by *ab. initio.* calculations as well as experiments. However, prior calculations on metal clusters have shown that relaxations were only compressions. Other significant behavior in the slabs is that, in contrast to the case of metal clusters, the  $E/N$  as a function of  $n$  converge to bulk value from above. In the asymptotic large  $n$  values, our results are in good agreement with those already obtained in semi-infinite calculations.

#### Acknowledgments

MP would like to highly appreciate professor John P. Perdew for his useful comments and discussion. This work is part of research program in NSTRI, Atomic Energy Organization of Iran.

#### APPENDIX: RELATION BETWEEN $r_s^\dagger$ AND $r_s^*$

The energy of the slab system is a function of volume,  $V$ , and  $r_s$ , *i. e.*,  $E = E(V, r_s)$ . In fact, instead of  $V$ , it depends on  $L$  because, in the slab system the surface area does not change. However, we use  $V$  for generality of our arguments. We define two different derivatives,  $D_N$  and  $D_V$ , which are derivatives when  $N$  is constant and when  $V$  is constant, respectively. That is,

$$\begin{aligned} D_N &\equiv \frac{d}{dr_s} \left[ \frac{E(V, r_s)}{N} \right]_N = \frac{1}{N} \frac{d}{dr_s} [E(V, r_s)]_N \\ &= \frac{4\pi}{3V} r_s^3 \frac{d}{dr_s} [E(V, r_s)]_N, \end{aligned} \quad (\text{A.1})$$

$$\begin{aligned} D_V &\equiv \frac{d}{dr_s} \left[ \frac{E(V, r_s)}{N} \right]_V = \frac{1}{V} \frac{d}{dr_s} \left[ \frac{V}{N} E(V, r_s) \right]_V \\ &= \frac{4\pi}{3V} \frac{d}{dr_s} [r_s^3 E(V, r_s)]_V. \end{aligned} \quad (\text{A.2})$$

However, on the one hand, using Eq. (7) one obtains

$$\frac{dV}{dr_s} = \frac{3V}{r_s}, \quad (\text{A.3})$$

which results in

$$\begin{aligned} \frac{d}{dr_s} [E(V, r_s)]_N &= \left[ \left( \frac{\partial E}{\partial V} \right)_{r_s} \frac{dV}{dr_s} + \left( \frac{\partial E}{\partial r_s} \right)_V \right]_N \\ &= \frac{3}{r_s} V \left( \frac{\partial E}{\partial V} \right)_{r_s} + \left( \frac{\partial E}{\partial r_s} \right)_V, \end{aligned} \quad (\text{A.4})$$

and on the other hand, the constant volume conditions results in

$$\frac{d}{dr_s} [E(V, r_s)]_V = \left( \frac{\partial E}{\partial r_s} \right)_V. \quad (\text{A.5})$$

Now, combining Eqs. (A.1)-(A.5) one obtains

$$D_V(V, r_s) = D_N(V, r_s) + \frac{4\pi r_s^2}{V} \left[ E(V, r_s) - V \left( \frac{\partial E}{\partial V} \right)_{r_s} \right] \quad (\text{A.6})$$

By definition,

$$D_V(V, r_s^*) = 0, \quad (\text{A.7})$$

and

$$D_N(V, r_s^\dagger) = 0. \quad (\text{A.8})$$

Inserting Eqs. (A.7) and (A.8) into (A.6) results in

$$D_N(V, r_s^*) + \frac{4\pi r_s^{*2}}{V} \left[ E(V, r_s^*) - V \left( \frac{\partial E}{\partial V} \right)_{r_s^*} \right], \quad (\text{A.9})$$

and

$$D_V(V, r_s^\dagger) - \frac{4\pi r_s^{\dagger 2}}{V} \left[ E(V, r_s^\dagger) - V \left( \frac{\partial E}{\partial V} \right)_{r_s^\dagger} \right]. \quad (\text{A.10})$$

Taylor expansion of Eq. (A.9) around  $r_s^\dagger$  to linear term and using Eq. (A.8) and combining with (A.10) one obtains

$$r_s^* = r_s^\dagger - \frac{D_V(r_s^\dagger)}{\left[ \frac{\partial D_N(r_s^\dagger)}{\partial r_s^\dagger} + \frac{\partial D_V(r_s^\dagger)}{\partial r_s^\dagger} \right]}. \quad (\text{A.11})$$

Since the energy  $E/N$  is a convex function of  $r_s$ , both terms in the denominator of Eq. (A.11) are positive while the sign of the numerator is positive for  $r_s^* < r_s^\dagger$  and negative for  $r_s^* > r_s^\dagger$ .

---

\* Correspondent author: mpayami@aeoi.org.ir

<sup>1</sup> F. K. Schulte, Surf. Sci. **55**, 427 (1976).

<sup>2</sup> E. E. Mola and J. L. Vicente, J. Chem. Phys. **84**, 2876 (1986).

<sup>3</sup> I. Sarria, C. Henriques, C. Fiolhais, and J. M. Pitarke, Phys. Rev. B **62**, 1699 (2000).

<sup>4</sup> J. P. Perdew, H. Q. Tran, and E. D. Smith, Phys. Rev. B **42**, 11627 (1990).

<sup>5</sup> J. P. Perdew, M. Brajczewska, and C. Fiolhais, Solid State Commun. **88**, 795 (1993).

<sup>6</sup> M. Payami, Can. J. Phys. **82**, 239 (2004).

<sup>7</sup> M. Payami, Phys. Rev. B **73**, 113106 (2006).

<sup>8</sup> P. Hohenberg and W. Kohn, Phys. Rev. **136**, B864 (1964).

<sup>9</sup> W. Kohn and L. J. Sham, Phys. Rev. **140**, A1133 (1965).

<sup>10</sup> J. L. F. Da Silva, Phys. Rev. B **71**, 195416 (2005).

<sup>11</sup> S. J. Sferco, P. Blaha, and K. Schwarz, Phys. Rev. B **76**, 75428-1 (2007).

<sup>12</sup> G. Materzanini, P. Saalfrank, and P. J. D. Lindan, Phys. Rev. B **63**, 235405 (2001).

<sup>13</sup> N. Zare and M. Payami, Int. J. Mod. Phys. C **19**, (2008).

<sup>14</sup> M. Payami, J. Phys. Condens. Matter **13**, 4129 (2001).

<sup>15</sup> M. Payami and T. Mahmoodi, J. Phys. Condens. Matter **18**, 75 (2006).

<sup>16</sup> N. W. Ashcroft, Phys. Lett. **23**, 48 (1966).